EurJIC European Journal of Inorganic Chemistry

SHORT COMMUNICATION

DOI: 10.1002/ejic.201200632

An Air-Stable Fe_3S_4 Complex with Properties Similar to Those of the H_{OX}^{air} State of the Diiron Hydrogenases

Yong Huang,[a] Weiming Gao,*[a] Torbjörn Åkermark,[b] Mingrun Li,[c] and Björn Åkermark*[d]

Keywords: Enzyme models / Electrochemistry / Iron / Proton reduction / Electron transfer

A Fe_3S_4 complex bridged by azapropanedithiolate (adt), complex **6**, was prepared as a potential model of the H_{OX}^{air} state of [FeFe]-hydrogenases. Complex **6** was characterized by IR and ^1H NMR spectroscopy, and its structure was determined by X-ray crystallography. The electrochemical studies show that complex **6** is redox-active under acidic conditions, which provides insight into the catalytic mechanism. Hydrogen evolution, driven by visible light, was observed in CH_3CN/D_2O solution by online mass spectroscopy.

Introduction

[FeFe]-hydrogenases have attracted considerable attention from the modeling community because of their exceptional efficiency in proton reduction.[1] The mechanisms for proton reduction and the reverse, hydrogen oxidation, have been extensively studied, and three different oxidation states have been identified, frequently named H_{red}, H_{OX}, and H_{OX}^{air}. It appears that the H_{OX}^{air} state is inactive in catalysis but is activated by one-electron reduction to the H_{OX} state. This, in turn, may be reversibly deactivated by CO to give H_{OX}^{CO}. The oxidation states are probably Fe (I,I), Fe(I,II), and Fe(II,II), respectively.[1] While the H_{red} and H_{OX} states have been well characterized, this is not true for

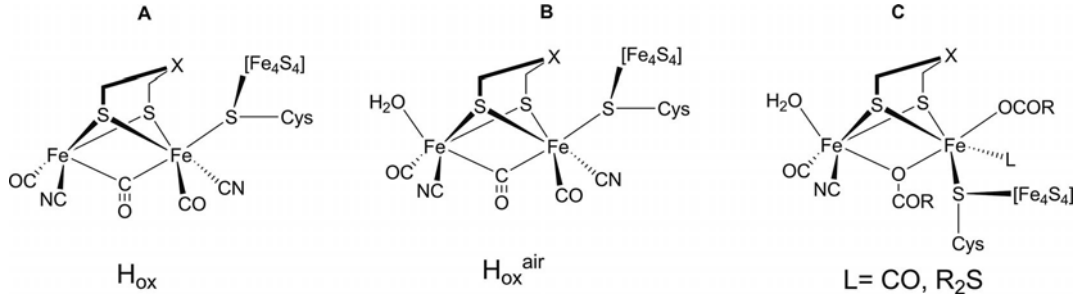

Figure 1. Structures proposed for the three states of the active site of [FeFe]-hydrogenase: **A** (for H_{OX}), **B** (for H_{OX}^{air}), and **C** (potential model for H_{OX}^{air}).

[a] Shenzhen Key Lab of Nano-Micro Material Research, Laboratory of Chemical Genomics, School of Chemical Biology and Biotechnology, Shenzhen Graduate School of Peking University,
Shenzhen 518055, China
Fax: +86-755-26033070
E-mail: gaowm@pkusz.edu.cn
Homepage: http://www.scbb.pkusz.edu.cn/huang/index.asp
[b] Applied Electrochemistry, School of Chemical Science and Engineering, Royal Institute of Technology (KTH),
10044 Stockholm, Sweden
[c] Division of Structural Chemistry, Arrhenius Laboratory, Stockholm University,
10691 Stockholm, Sweden
[d] Department of Organic Chemistry, Arrhenius Laboratory, Stockholm University,
10691 Stockholm, Sweden
E-mail: bjorn.akermark@organ.su.se
Homepage: www.organ.su.se/ba

the H_{OX}^{air} state. This is important, because this state is air-stable and perhaps serves to protect hydrogenases from destruction by air. Further modeling is thus of interest. According to some reports, the H_{OX} and H_{OX}^{air} states contain a bridging CO (**A** and **B** in Figure 1). With reference to these data, Rauchfuss and co-workers have presented a series of models in which the bridge is isocyanide or carbon monoxide.[2] They have also been able to show that such models are capable of strongly catalyzing the oxidation of hydrogen with a mild oxidant such as ferrocenium ions.[3]

However, the isolation of complex **6** suggests that there may be alternative possibilities for the structure of H_{OX}^{air}. In fact, a theoretical study of Fe(II,II) model complexes indicates that a terminally coordinated water or hydroxide

may replace CO as bridge in such complexes for thermodynamic reasons.[4] On the basis of complex **6**, we therefore propose a second potential model **C** for H_{OX}^{air}, with a structure related to complex **B** but lacking the bridging CO.

Results and Discussion

In previous work,[5] we reported on the synthesis of the carboxylate-substituted diiron(I) azadithiolate (adt) complex **1** containing two PMe_3 ligands. On protonation with strong acid, the bridged Fe(II,II) hydrides **2′**and **2** were formed. It had earlier been proposed that the protonated nitrogen of the adt bridge could participate, by hydrogen bonding, in a primarily formed iron hydride and serve to protonate the hydride to produce molecular hydrogen.[6] We therefore assumed that hydrogen bonding to the carboxylate might help to increase the mobility of the proton attached to the nitrogen and aid in the initial formation of an iron hydride and in its protonation to yield molecular hydrogen.[5] We have now found that, when complex **1** is treated with excess HBF_4 (20 equiv.), hydrogen is generated spontaneously, and the air-stable trinuclear iron(II) complex **6** is formed in approximately 30% yield. A tentative mechanism is shown in Scheme 1. The proposed intermediate, compound **4**, reacts with itself to form tetranuclear complex **5** after attack of carboxylate and sulfur on the future central iron, with simultaneous migration of CO. Another attack by sulfur is then followed by the migration of a second CO and loss of $Fe(CO)_4(PMe_3)_2^{2+}$ to give complex **6**. The evolution of hydrogen was confirmed by online GC–MS measurements. The shift of the IR peaks for the carbonyl bonds of the carboxyl groups from 1659 cm^{-1} in **1** to 1634 cm^{-1} in **6** is in agreement with their coordination as carboxylates to the central iron atom.

The crystal structure of trinuclear complex **6** is shown in Figure 2 together with the atomic labeling system. In principle, it consists of two connected dinuclear models for the H_{OX}^{air} state, where the central iron on both sides is connected to an iron(CO, PMe_3) unit by one bridging carboxylate oxygen and an adt bridge. Selected crystal data are summarized in Table 1 and compared to the H_{OX}^{CO} state analogues $[Fe_2(S_2C_3H_6)(\mu\text{-}CO)(CNMe)_6](PF_6)_2$ (**7**) and $[Fe_2(S_2C_3H_6)(\mu\text{-}CNMe)(CO)(CNMe)_5](PF_6)_2$ (**8**).[2b]

Individually, each Fe_2S_2 subunit of complex **6** has a square-pyramidal structure. The Fe–Fe distance of **6** (2.992 Å) falls outside the range of the common Fe–Fe bond lengths for $Fe^{II}{}_2$ model complexes bridged by CO or hydride (usually, 2.5–2.6 Å).[1g,2,7] However, there are a number of reported Fe_2(II,II) complexes that are either bridged only by an adt or related bridge or bridged by di-

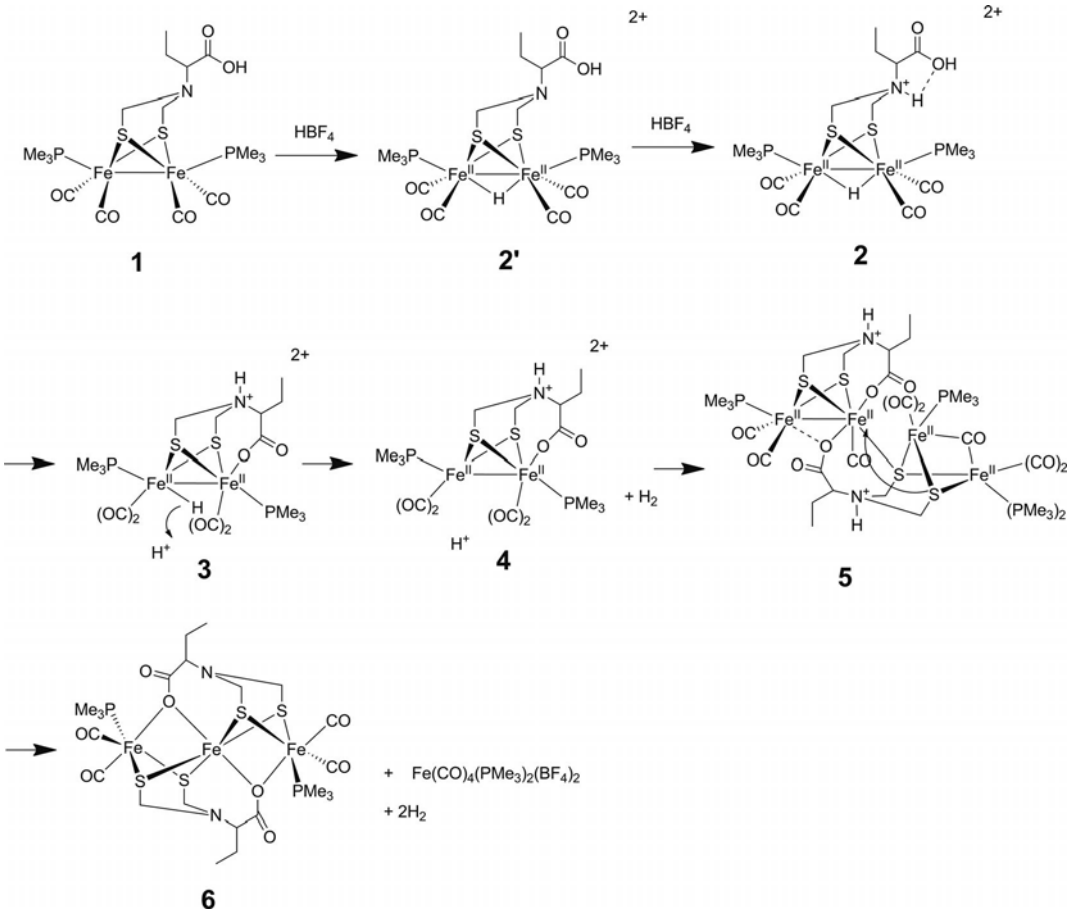

Scheme 1. Formation of complex **6**.

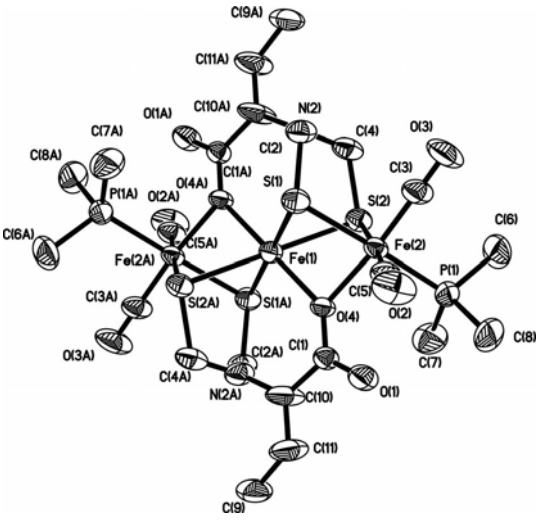

Figure 2. ORTEP (ellipsoids at 50% probability) diagram of complex **6**.

Table 1. Selected metric data.[a]

	6	**7**	**8**	Active site of *C. Pasteuriamum*
Fe(1)–Fe(2)	2.992[b]	2.503	2.629	2.61
Fe(1)–S(1)	2.511	2.259	2.296	2.34
Fe(1)–S(2)	2.513	2.260	2.297	2.31
Fe(2)–S(1)	2.351	2.268	2.273	2.31
Fe(2)–S(2)	2.335	2.231	2.244	2.33

[a] Bond lengths in Å. [b] The nonbonding distance.

sulfide and chloride[8a] or a third sulfide,[8b] which yield Fe–Fe bond lengths around 3 Å, close to the nonbonding value observed for complex **6**.

The sum of the angles at the bridge N atom of **6** is 360°, suggesting sp^2 hybridization, which, together with the twisted/locked aliphatic carboxylate chain, makes direct protonation on nitrogen difficult. The angle Fe(2)–O4–Fe(1) of 92.8° indicates two almost vertical Fe–O bonds. The PMe_3 ligands occupy basal positions for steric reasons. The crystal structure of **6** shows that, as anticipated previously,[5a] the carboxyl group in complex **1** can interact with the iron cluster, in principle affording a mechanism for proton-coupled electron reduction of the complex, assisted by the carboxyl group.

Complex **6** displayed two reduction peaks at approximately –1.28 and –1.60 V vs. Fc/Fc^+. On addition of HBF_4, the current at the first reduction peak grew linearly with increasing amount of acid (Figure 3). The peaks also shifted slightly to more negative potential. These features are indicative of the presence of a catalytic proton reduction.[8c,8d] A curve-crossing peak at approximately –1.3 V was observed upon addition of more than three equivalents of acid. All the reduction peak currents (ip) were plotted against scan rates from 100 to 800 mV/s; a square-root relationship between ip and the scan rate was obtained, which is an indication that the "curve-crossing" peak is not the result of a surface deposition process,[8c,8e] and confirms that the current is diffusion-controlled. For **6**, The implications of the curve crossing are not clear but suggest that a chemical reaction, for example reductive elimination of hydrogen, takes place to give an intermediate, which is oxidized at the crossing, at approximately –1.3 V. In the absence of complex **6**, proton reduction does not start until a potential of approximately –2 V, with relatively low current intensity.[5a,8c] Complex **6** is stable in acid solution over a period of at least 24 h.

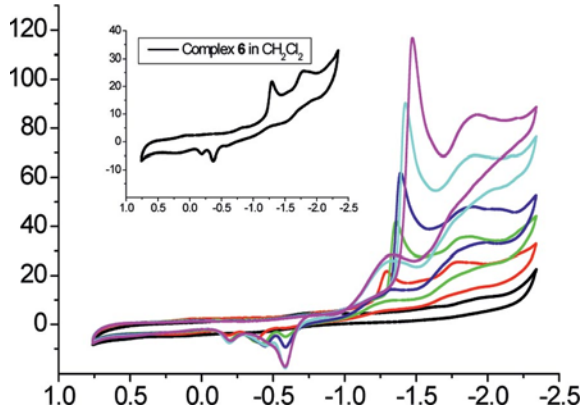

Figure 3. Cyclic voltammetry of complex **6** (1 mM) in 0.05 M nBu_4NPF_6/CH_3CN in the absence and presence of HBF_4 at a scan rate of 100 mV/s. In the absence of complex **6**, hydrogen evolution starts at a potential below –2 V vs. Fc/Fc^+. Inset: CV of complex **6** neat in CH_2Cl_2 solution.

Light-driven hydrogen generation by complex **6** was studied in the presence of a $Ru(bpy)_3^{2+}$ sensitizer in CH_3CN/D_2O solution.[5a] The MS analysis of the evolved hydrogen (H_2, HD, and D_2) showed that it is indeed formed by reduction of protons in water. Another important feature is that carbon monoxide was detected. This could explain the low turnover number (TN) for hydrogen evolution (ca. 0.2), since it shows that complex **6** undergoes photoinduced decomposition in the absence of a sacrificial donor.

So far there is no structure reported for the inactive H_{OX}^{air} state; the early structural study by Peters and coworkers shows that the oxidized form of the enzyme from *Clostridium* can be bridged both by CO and water, the bridging CO appearing at approximately 1850 cm^{-1}.[9a] In our case, the frequencies for complexes **1** [Fe(I,I), (1978, 1941, 1898 cm^{-1})], **2′** [Fe(II,II), (2046, 2007 cm^{-1})], **2** [Fe(II,II), (2032, 1993 cm^{-1})], and **6** [Fe(II,II,II), (2032, 1992 cm^{-1})] show no bridging CO ligand. However, the data for complexes **2′** and **6** indicate the presence of terminal carbonyl groups, as in H_{OX}^{air} from *Desulfovibrio vulgaris*, at 2007 and 1983 cm^{-1}.[9b]

There is a site at the terminal iron that is probably occupied by water in the active enzyme but displaced by additional CO. This raises the carbonyl frequencies to 2016 and 1972 also for this species, which is probably Fe(I,II) (H_{OX}) in contrast to H_{OX}^{air}, which is very likely Fe(II,II). Also **6**, which is clearly an Fe(II,II) complex, has a similar frequency pattern at the terminal Fe, but lacks the bridging CO. The carbonyl IR frequencies of complex **6** at 2032 and 1992 cm^{-1} are characteristic of iron(II) complexes.

Conclusions

Complex **6**, a trinuclear complex that has spectroscopic properties similar to the H_{OX}^{air} state of the active site of [FeFe]-hydrogenases, was isolated. In this complex, carboxylate groups replace CO as bridges between the iron atoms. The crystal structure of complex **6** was determined by X-ray diffraction. The electrochemical and photoinduced evolution of hydrogen is promoted by this Fe_3S_4 catalyst. In principle, this opens a route to the construction of new types of dinuclear hydrogenase models, such as compound **C**. One could imagine that, during oxidation of the iron from Fe (I,I) to Fe(II,II), bridging CO is replaced by an external carboxylate function. Since carboxylate functions are provided by amino acid neighbors, such a scenario for protection of the active hydrogenases against further oxidation seems reasonable.

Experimental Section

General Remarks

Unless otherwise indicated, all reactions and operations related to organometallic complexes were carried out under a dry, oxygen-free argon atmosphere with standard Schlenk techniques. Chemicals were purchased from Aldrich, and all solvents were dried and distilled prior to use according to the standard methods.

Infrared spectra were recorded with a Perkin–Elmer Spectrum One instrument. NMR spectra were collected with a Varian spectrometer (400 MHz). The elemental analyses were performed at the Analytische Laboratorien GmbH, Lindlar, Germany. Electrospray mass spectrometry was performed with a Bruker Daltonics BioAPEX-94e superconducting 9.4 T FTICR mass spectrometer (Bruker Daltonics, Billerica, MA, USA) (FTICR-ESI MS).

Acetonitrile (Aldrich, spectroscopy grade), which was used in the electrochemistry, was dried with molecular sieves (4 Å) and then freshly distilled from CaH_2 under an argon atmosphere. A solution (0.05 M) of nBu$_4$NPF$_6$ (Fluka, electrochemical grade) in CH_3CN was used as electrolyte. Electrochemical measurements were carried out in a three-electrode cell connected to an Autolab potentiostat with a GPES electrochemical interface. The working electrode was a glassy carbon disc (diameter 2 mm, freshly polished). The reference electrode was a nonaqueous Ag/Ag$^+$ electrode (1.0 mM $AgNO_3$ in CH_3CN) with the ferrocene/ferrocenium (Fc/Fc$^+$) couple as an external standard. The auxiliary electrode was a platinum wire. All potentials reported here are quoted relative to the Fc/Fc$^+$ couple. The solutions were purged with solvent-saturated argon to remove residual oxygen. All experimental measurements were carried out under an atmosphere of argon at all times.

Complex 6: A solution of complex **1** (0.057 g, 0.1 mmol) in DCM (2 mL) was added to HBF_4/Et_2O (0.15 mL) in a Schlenk bottle. Hydrogen evolution was measured with mass spectrometry as described earlier.[5a] The mixture was allowed to react at room temperature for several hours, until complex **1** was consumed, as monitored by IR spectroscopy. Alternatively, the reaction could be performed under an air atmosphere. This gave a slightly more rapid reaction but essentially the same yield of product. The solvent was removed, and the crude product was purified by column chromatography with hexane/CH_3COCH_3/CH_2Cl_2 as eluent to give **6** (23 mg, 27%). ^{1}H NMR (CD_3CN): δ = 1.43 (t, J = 6.9 Hz 6 H, CH_2CH_3), 1.53 (m, 4 H, $CHCH_2CH_3$), 1.61 (m, 18 H, PCH_3), 3.51 (s, 2 H, $CH_2CHNCOO$), 3.57 (s, 4 H, 2× NCH_2S), 3.68 (s, 4 H, 2× NCH_2S) ppm. ^{31}P NMR (CD_3CN): δ = 20.3 ppm. IR (CH_2Cl_2): $\tilde{\nu}$(CO) = 2032, 1992, 1634 cm^{-1}. $C_{22}H_{38}Fe_3N_2O_8P_2S_4$ (816.28): calcd. C 32.37, H 4.69, N 3.43; found C 32.39, H 4.70, N 3.46.

Structure Determination

Single-crystal X-ray diffraction patterns were recorded with an Oxford Diffraction Excalibur diffractometer equipped with a sapphire-3 CCD on a Mo-radiation source (λ = 0.71073 Å) with ω scans at different ϕ values to fill the Ewald sphere. The sample–detector distance was 50 mm. The maximum 2θ was approximately 63°.

Indexing, cell refinements, and integration of reflection intensities were performed with the CrysAlis software.[10] Numerical absorption correction was performed with the program X-RED,[11] and the crystal shape was verified with the program X-shape.[12] The structure was solved by direct methods with SHELXS97[13] to give electron density maps in which most of the non-hydrogen atoms could be resolved. The rest of the non-hydrogen atoms were located from difference electron density maps, and the structure model was refined with full-matrix least-squares calculations on $F2$ by using the program SHELXL97–2.[14] All non-hydrogen atoms were refined with anisotropic displacement parameters, while the hydrogen atoms, which were placed in geometrically calculated positions and allowed to ride on the atoms to which they were bonded, were given isotropic displacement parameters calculated as ξU_{eq} for the non-hydrogen atoms, with ξ = 1.2 for methylene (–CH_2–) and aromatic hydrogen atoms.

CCDC-878422 contains the supplementary crystallographic data for this paper. These data can be obtained free of charge from The Cambridge Crystallographic Data Centre via www.ccdc.cam.ac.uk/data_request/cif.

Photochemical Hydrogen Generation

The mass spectrometer setup (MS-setup), including the reactor, has been described earlier[5a,15–19] (see Figure 4). This makes it possible to quantitatively determine small amounts of produced gases with masses in the interval 1–100 mass units. The light source was a 150 W halogen lamp. Since we used a glass reactor, no UV filter was necessary, as shown by the fact that the use of a Pyrex glass UV filter had no effect on the reactions.

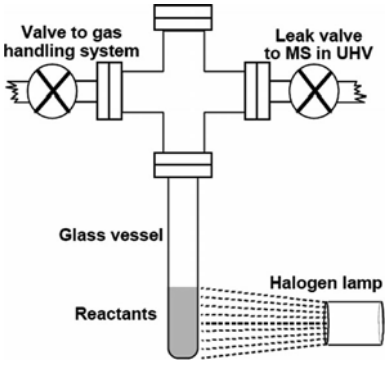

Figure 4. Experimental setup for determination of photochemical hydrogen generation.

Complex **6** (5 μmol) was dissolved in a mixture of deuterated water and acetonitrile (1:1, 5 mL) and HBF_4 (1 mmol) was added. The system was closed and then evacuated for 5 min to remove dissolved gases. Argon (ca. 30 mbar) was introduced and the inlet to

the MS was adjusted. When the partial pressures in the MS were stable after approximately 10 min, the light was turned on and the evolution of H_2 and CO was monitored. Since no sacrificial donor was used, the yield of H_2 was low, approximately 20%. The reason is decomposition of the complex, as shown by generation of approximately 15 μmol of CO.

Acknowledgments

We thank the Shenzhen Government Program (JC201005260103A) for financial support. We are also grateful to the Swedish Research Council, K&A Wallenberg Foundation, and the Swedish Energy Agency for the financial support of this work.

[1] a) A. L. De Lacey, V. M. Fernández, M. Rouset, R. Cammack, *Chem. Rev.* **2007**, *107*, 4304–4330; b) P. M. Vignais, B. Billoud, *Chem. Rev.* **2007**, *107*, 4206–4272; c) G. J. Kubas, *Chem. Rev.* **2007**, *107*, 4152–4205; d) W. Lubitz, E. Rejerse, M. Van Gastel, *Chem. Rev.* **2007**, *107*, 4331–4365; e) J. C. Fontecilla-Camps, A. Volbeda, C. Cavazza, Y. Nicolet, *Chem. Rev.* **2007**, *107*, 4273–4303; f) F. Gloaguen, T. B. Rauchfuss, *Chem. Soc. Rev.* **2009**, *38*, 100–108; g) C. Tard, C. J. Pickett, *Chem. Rev.* **2009**, *109*, 2245–2274; h) P. E. M. Siegbahn, J. W. Tye, M. B. Hall, *Chem. Rev.* **2007**, *107*, 4414–4435.

[2] a) A. K. Justice, M. J. Nilges, T. B. Rauchfuss, S. R. Wilson, L. D. Gioia, G. Zampella, *J. Am. Chem. Soc.* **2008**, *130*, 5293–5301; b) C. A. Boyke, T. B. Rauchfuss, S. R. Wilson, M.-M. Rohmer, M. Bénard, *J. Am. Chem. Soc.* **2004**, *126*, 15151–15160; c) J. D. Lawrence, T. B. Rauchfuss, S. R. Wilson, *Inorg. Chem.* **2002**, *41*, 6193–6195.

[3] a) J. M. Camara, T. B. Rauchfuss, *J. Am. Chem. Soc.* **2011**, *133*, 8098–8101; b) J. M. Camara, T. B. Rauchfuss, *Nature Chem.* **2011**, *4*, 26–30; c) M. T. Olsen, T. B. Rauchfuss, S. R. Wilson, *J. Am. Chem. Soc.* **2010**, *132*, 17733–17740.

[4] M. Bruschi, P. Fantucci, L. De Gioia, *Inorg. Chem.* **2003**, *42*, 4773–4781.

[5] a) W. Gao, J. Sun, T. Åkermark, M. Li, L. Eriksson, L. Sun, B. Åkermark, *Chem. Eur. J.* **2010**, *16*, 2537–2546; b) W. Gao, J. Sun, M. Li, T. Åkermark, K. Romare, L. Sun, B. Åkermark, *Eur. J. Inorg. Chem.* **2011**, 1100–1105.

[6] a) J.-F. Capon, S. Ezzaher, F. Gloaguen, F. Y. Pétillon, P. Schollhammer, J. Talarmin, *Chem. Eur. J.* **2008**, *14*, 1954–1964; b) B. E. Barton, M. T. Olsen, T. B. Rauchfuss, *J. Am. Chem. Soc.* **2008**, *130*, 16834–16835.

[7] a) J. W. Peters, W. N. Lanzilotta, B. J. Lemon, L. C. Seefeldt, *Science* **1998**, *282*, 1853–1858; b) Y. Nicolet, C. Piras, P. Legrand, C. H. Hatchikian, J. C. Fontecilla-Camps, *Structure* **1999**, *7*, 13–23; c) Y. Nicolet, A. L. de Lacey, X. Verne'de, V. M. Fernandez, E. C. Hatchikian, J. C. Fontecilla-Camps, *J. Am. Chem. Soc.* **2001**, *123*, 1596–1601; d) M. Schmidt, S. M. Contakes, T. B. Rauchfuss, *J. Am. Chem. Soc.* **1999**, *121*, 9736; e) S. L. Mattews, D. M. Heinekey, *Inorg. Chem.* **2010**, *49*, 9746–9748; f) M. Y. Darensbourg, *Inorg. Chem.* **2002**, *41*, 3917–39028; g) C. A. Boyke, J. I. van der Vlugt, T. B. Rauchfuss, S. R. Wilson, G. Zampella, L. De Goia, *J. Am. Chem. Soc.* **2005**, *127*, 11010–11018.

[8] a) S. L. Matthews, D. M. Heinekey, *Inorg. Chem.* **2011**, *50*, 7925–7927; b) V. E. Kaassjager, R. K. Henderson, E. Bouwman, M. Lutz, A. L. Spek, J. Reedijk, *Angew. Chem.* **1998**, *110*, 1787; *Angew. Chem. Int. Ed.* **1998**, *37*, 1668–1670; c) W. Gao, J. Liu, B. Åkermark, L. Sun, *Inorg. Chem.* **2006**, *45*, 9169–9171; d) F. Gloaguen, J. D. Lawrence, T. B. Rauchfuss, M. Benard, M.-M. Rohmer, *Inorg. Chem.* **2002**, *41*, 6573–6582; e) R. Meijia-Rodriguez, D. Chong, J. H. Reibenspies, M. P. Soriaga, M. Y. Darensbourg, *J. Am. Chem. Soc.* **2004**, *126*, 12004–12014.

[9] a) B. J. Lemon, J. W. Peters, *Biochemistry* **1999**, *38*, 12969–12973; b) A. M. Pierik, M. Hulstein, W. R. Hagen, S. P. J. Albracht, *Eur. J. Biochem.* **1998**, *258*, 572–578.

[10] *CrysAlis Software System*, version 1.170, Oxford Diffraction Ltd., Oxford, **2003**.

[11] *X-RED, Absorption Correction Program*, version 1.09, Stoe & Cie GmbH Darmstadt, Darmstadt.

[12] *X-SHAPE, Crystal Optimisation for Numerical Absorption Correction*, version 1.2, Stoe & Cie GmbH Darmstadt, Germany.

[13] G. M. Sheldrick, *Acta Crystallogr., Sect. A* **1990**, *46*, 467–473.

[14] G. M. Sheldrick, *SHELXL97–2, Computer Program for the Refinement of Crystal Structures*, University of Göttingen, Göttingen, **1997**.

[15] G. Hultquist, L. Gråsjö, Q. Lu, T. Åkermark, *Corros. Sci.* **1994**, *36*, 1459–1471.

[16] T. Åkermark, J.-J. Ganem, I. Trimaille, S. Rigo, *J. Electrochem. Soc.* **1999**, *146*, 4580–4585.

[17] T. Åkermark, B. Emmoth, H. Bergsåker, *J. Nucl. Mater.* **2006**, *359*, 220–226.

[18] C. Anghel, Q. Dong, *J. Mater. Sci.* **2007**, *42*, 3440–3453.

[19] Y. Xu, T. Åkermark, V. Gyollai, D. Zou, L. Eriksson, L. Duan, R. Zhang, B. Åkermark, L. Sun, *Inorg. Chem.* **2009**, *48*, 2717–2719.

Received: June 11, 2012
Published Online: August 17, 2012

